Synthesis and Characterization of Carboxymethyl Cellulose from Oil Palm Empty Fruit Bunch Stalk Fibres

Dzieda Muhamad Parid, Nur 'Aliaa Abd Rahman,* Azhari Samsu Baharuddin, Mohd Afandi P. Mohammed, Amiruddin Mat Johari, and Siti Zubaidah Abdul Razak

The current extraction of carboxymethyl cellulose (CMC) from wood has created competition with wood industries. Interest in alternative sources is critical to ensure the sustainable production of CMC. Therefore, the extraction of CMC from oil palm empty fruit bunch (OPEFB) stalk fibres was evaluated. CMC extracted from OPEFB stalk fibres was characterized for chemical composition as well as by spectroscopic, microscopic, physicochemical, and rheological tests. Highest cellulose content was obtained from raw stalk fibres with the least amount of lignin and residual oil as compared to the empty fruit bunch (EFB) and spikelet. The XRD analysis revealed that the native cellulose was transformed into an amorphous phase, as evidenced from the characteristic peaks that had almost disappeared. Likewise, the FTIR analysis showed that major peaks in the lignin and hemicellulose were absent, which enabled the cellulose to be converted to CMC. Microscopy analysis showed notable changes in the fibres' morphology throughout the extraction process. In addition, X-ray diffraction (XRD), Fourier transform infrared (FTIR), scanning electron microscopy (SEM), physicochemical studies, and rheological tests on extracted CMC showed that there was a significant difference between each phase of the extraction process and this showed that OPEFB stalk fibre was feasible to produce CMC that was comparable to those of commercial CMC.

Keywords: Carboxymethyl cellulose (CMC); Oil palm empty fruit bunch (OPEFB); Stalk fibre

Contact information: Department of Process and Food Engineering, Faculty of Engineering, Universiti Putra Malaysia, 43400 UPM, Serdang, Selangor, Malaysia;
** Corresponding author: nuraliaa@upm.edu.my*

INTRODUCTION

Palm oil mills produce a few types of solid wastes, one of which is called oil palm empty fruit bunch (OPEFB). During the threshing process, the fresh fruit bunches (FFB) are rolled and threshed in rotating steel drums to separate the fruits from the stalks, and this process generates the empty fruit bunches (EFB). Attempts to transform OPEFB into value-added products have gained wide attention because it is one of the most produced biomasses that come from oil palm refineries. The lignocellulosic composition in the dry OPEFB was 19% to 21% for lignin, 22% to 25% for hemicellulose, and 40% to 43% for cellulose (Razali *et al.* 2017).

The two main parts of OPEFB are the stalk and spikelet, where Xiang *et al.* (2016) reported that the raw stalk fibre yielded the highest cellulose content and had the lowest lignin content. Likewise, the raw stalk fibre contains the lowest residual oil content when compared to the EFB and spikelets (Yunos *et al.* 2015; Xiang *et al.* 2016). The supplemental pre-treatment step during the extraction of cellulose and its derivatives is required to remove the residual oil present in oil palm fibres because it can influence the cellulose derivatives production (Fahma *et al.* 2010). Furthermore, Xiang *et al.* (2016) investigated the cellulose percentage of microcrystalline cellulose (MCC), where the MCC extracted from stalk contained a greater amount of cellulose. This amount is 86.5% compared to those MCC extracted from OPEFB and spikelets that consisted of 81.1% and 84.5%, respectively. Because the spikelets was surrounded by the fruitlets, which were the main source of oil, they contained a higher amount of residual oil.

Cellulose must be transformed into its derivatives to be used in the food industry, such as carboxymethyl cellulose (CMC). Thus, no report on utilizing the raw OPEFB stalk fibres to produce carboxymethyl cellulose (CMC) is currently available. CMC can be described as a linear, water soluble, long-chain, anionic polysaccharide that is produced by the reaction of alkali-treated cellulose with monochloroacetate (Tasaso 2015). It is white to cream color, tasteless, odorless, and typically provided as a free-flowing powder (Adinugraha *et al.* 2005). It is used in a variety of industries including foods, detergents, and pharmaceuticals (Tasaso 2015).

The purpose of this work was to characterize each phase of the extraction process through lignocellulosic, spectroscopic, and microscopic analyses. The production of CMC from raw OPEFB stalk fibres was conducted by using a chemical extraction method, prior to proceeding with the physicochemical and rheological analyses of the extracted CMC. A comparison was made between the CMC produced in this study with those commercially available. The current research provided the first step towards clean OPEFB stalk fibre as a source to produce CMC.

EXPERIMENTAL

Materials

The OPEFB were obtained after the threshing process from the Felda Sungai Tengi palm oil mill (Selangor, Malaysia). The OPEFB were placed in a deep freezer at -20 °C to inhibit fungal contamination. The OPEFB stalks were then isolated manually to remove the spikelets. Then, the stalk fibres were shredded manually from the stalk bundle before being cleansed with a 2% detergent solution and rinsed with tap water to remove any of the remaining dust and oil. Afterwards, the clean OPEFB stalks were oven-dried at 60 °C for 24 h. A power-cutting mill (Retsch Technology GmbH, SM 200, Haan, Germany) was used to cut the dried OPEFB stalk fibres into a 0.2 mm powdered form.

Isolation of α-cellulose

A 0.7% (w/v) sodium chlorite ($NaClO_2$) solution was used to treat a mixture of 10 bunches of powdered OPEFB stalk fibres collected after the threshing process. Acetic acid was added until the pH reached 4 to acidify the sodium chlorite ($NaClO_2$) solution. The acidified $NaClO_2$ solution with a fibre:$NaClO_2$ ratio of 1:50 (g/mL^{-1}) was prepared to bleach the fibres by heating the fibres at 70 °C to 80 °C for 2 h. The bleaching process was done repeatedly five times. After the bleaching process, distilled water was used to wash and rinse the residues to remove the yellowish color and odor from the chlorine oxide. The samples were allowed to dry at 60 °C overnight. Bleached fibres were then treated with 17.5% (v/v) sodium hydroxide (NaOH) solution with a fibre:NaOH solution ratio of 1:25 (g/mL^{-1}) for 2 h at room temperature. Lastly, the mixture was then filtered, washed, and oven-dried at 60 °C for 24 h, which produced the α-cellulose fibres (Xiang *et al.* 2016).

Synthesis of Carboxymethyl Cellulose

Approximately 5.0 g of cellulose was measured and placed into a 250-mL container. Then, 10 mL of 30% (v/v) sodium hydroxide was added drop-wise, which was followed by adding 100 mL of isopropyl alcohol as the solvent. The mixture was mechanically stirred at room temperature for 1 h for an alkalization process. This step is to make the cellulose easier to react during the carboxymethylation process. After the alkalization process, the carboxymethylation process began by adding 6.0 g of monochloroacetate (MCA; BIS Chemicals, Shah Alam, Malaysia) per 5.0 g cellulose, where the temperature of the reaction mixture was raised up to 45 °C and the reaction continued for 3 h. The mixture was then filtered, and the slurry was soaked in 300 mL of absolute methanol overnight to remove impurities. Glacial acetic acid was used to neutralize the suspended methanol solution, and then the mixture was sieved. The purification step commenced by washing the solid that was obtained by using 70% ethanol followed by 99.7% ethanol, three times to eliminate the undesirable by-products. The CMC obtained was to a constant weight at 60 °C (Pushpamalar *et al.* 2006).

Characterization of sodium carboxymethyl cellulose-lignocellulosic compositions

Neutral detergent fibre (NDF), acid detergent fibre (ADF), and acid detergent lignin (ADL) method analyses were completed to determine the cellulose, hemicellulose, and lignin contents, as described by Mohammed *et al.* (2012). The NDF content was determined by refluxing the sample in a boiling neutral reagent for 1 h. Then, the solution was cooled and filtered. The residues were washed with distilled water and acetone prior to the drying process. A different detergent solution was used, known as an acid detergent solution for the ADF analysis. The ADL content was then measured by hydrolyzing the remaining fibres from the ADF analysis with 72% (w/v) sulphuric acid. The fibres were washed and dried before being ignited in a furnace. The difference between the initial and final weight was calculated to determine the percentage of NDF, ADF, and ADL. The equations used to calculate the percentage of cellulose, hemicellulose, and lignin are as follows:

$$\text{Cellulose (\%)} = \text{ADF} - \text{ADL} \qquad (1)$$

$$\text{Hemicellulose (\%)} = \text{NDF} - \text{ADF} \qquad (2)$$

$$\text{Lignin (\%)} = \text{ADL} \qquad (3)$$

X-ray diffractometry

An X-ray diffractometer (Shimadzu, XRD6000, Tokyo, Japan) was used to determine the crystallinity of the samples by using a CuK_α radiation. The sample was scanned and the intensity was recorded in a 2θ range from 10° to 30°. The crystallinity index (CrI) of the sample was computed based on the formula proposed by Segal *et al.* (1959),

$$CrI = [(I_{002} - I_{\text{am}}) \,/\, I_{002}] \times 100 \qquad (4)$$

where I_{002} is the maximum intensity of the lattice diffraction at 2θ and is between 22° to 23° for cellulose I and between 18° and 22° for cellulose II, I_{am} is the minimum intensity of lattice diffraction attributed to amorphous cellulose at 2θ between 18° to 19° for cellulose I and between 13° and 15° for cellulose II (Roncero *et al.* 2005).

FT-IR spectroscopy

The FTIR spectra of OPEFB stalk fibres throughout the CMC extraction processes were obtained using FTIR to determine the chemical changes caused by the extraction processes. The samples were scanned in a range from 500 cm^{-1} to 4000 cm^{-1} with a resolution of 4 cm^{-1} with a total of 32 scans for each sample.

Scanning electron microscopy

The surface morphology changes of OPEFB stalks throughout CMC extraction processes were observed through SEM (Hitachi, S-3400N, Tokyo, Japan). A 10-mm sample was mounted on a gold stub and sputter-coated (EMITECH, K550X, Quorum Technologies Ltd, East Sussex, UK) with platinum prior to the morphological assessment. The voltage used was 5 kV throughout the scanning process.

Physicochemical properties of synthesized Na-CMC

The moisture content, density of powders, water retention capacity, color analysis, pH value, solubility, foam formability, and organoleptic properties were determined for the physicochemical characterization.

Moisture content

Approximately 5 g of the synthesized CMC was weighed to the nearest 0.001 g in a tared and covered weighing bottle. Then, the sample bottle was placed in an oven at 105 °C for 2 h with the cover removed. After 2 h, the bottle was cooled in a desiccator, the cover was replaced, and then the specimen in its bottle was weighed. The procedure was continued to a mass loss of not more than 5 mg for 30 min drying time. Lastly, the sample residues were weighed and the overall steps continued for triplicate readings. The percent moisture (*M*) was calculated as follows (ASTM D1439-03, 2008),

$$M = \left(\frac{A}{B}\right) X\ 100 \tag{5}$$

where *A* is mass loss on heating (g) and *B* is the mass of the sample that was used (g).

Density of CMC powders

Three types of densities were determined that were true density, bulk density, and tapped density. The true density of each sample of CMC powders were measured using helium pycnometry (Accupyc II 1340 Pycnometer, Micromeritics Instrument Corp., Norcross, GA, USA). For bulk density, 2.5 g of samples of CMC powders were poured through a funnel into a dry 10-mL graduated cylinder. At least 60% of the cylinder was filled with sample. The untapped volume was read directly from the nearest graduated unit cylinder without compacting and tapping. The values were recorded. All of the steps continued to use different samples of CMC and were repeated three times for each sample. The bulk density was calculated using,

$$\rho_{\text{bulk}} = \mathrm{m} \,/\, \mathrm{v} \tag{6}$$

where p_{bulk} is the bulk density (g/mL), *m* is the powder mass (g), and *v* is the volume of untapped powder (mL). The tapped density for all of the samples was determined using an Automatic Envelope (Bulk) Density Analyzer (Geopyc Model 1360, Micromeritics Instrument Corp., Norcross, GA, USA). The samples were analyzed 3 times on average with the equipment.

Hausner ratio and Carr index

The Hausner's Ratio for each sample of CMC powders were calculated as follows,

$$HR = p_{\mathrm{tapped}} \,/\, \rho_{\mathrm{bulk}} \qquad (7)$$

where *HR* is the Hausner ratio, p_{tapped} is the tapped density (g/cm^3), and p_{bulk} is the bulk density (g/cm^3) of CMC powders. Meanwhile, the Carr index (CI) was calculated using the following equation,

$$CI = [(\rho_{\mathrm{tapped}} - \rho_{\mathrm{bulk}}) \,/\, \rho_{\mathrm{tapped}}] \times 100 \qquad (8)$$

where *CI* is the Carr index, p_{tapped} is the tapped density (g/cm^3), and p_{bulk} is the bulk density (g/cm^3).

Water retention capacity (WRC)

For water and oil retention capacity tests, 25 mL of distilled water or commercial olive oil was added to 1 g of dry sample, stirred, and incubated at 40 °C for 1 h. After centrifugation, the residue was weighed, and the WRC was calculated as (Larrauri *et al.* 1996),

$$WRC\ (g/g) = \frac{wet\ weight - dry\ weight}{dry\ weight} \qquad (9)$$

Color

The color test was performed using a color spectrophotometer (HunterLab Ultrascan Pro, Reston, VA). The readings were taken three times. The Hunterlab color scale was used to determine the color of the materials. Meanwhile, for the color analysis, the Hunter color values (*L*, *a*, and *b*), yellowness index (YI), whiteness index (WI), and total color difference (ΔE) of the synthesized CMC stalk fibre were analyzed and compared with the commercial ones.

Foam formability and organoleptic properties

A foam formability test was conducted by shaking 0.1% CMC solution. Meanwhile, a physical examination was completed for the organoleptic properties test relating to qualities such as taste, color, odor, and feel of a substance.

Rheological testing

The rheological behavior of the extracted CMC from OPEFB stalk fibres was compared with commercial CMC (COMM1 from Warisnove, Pahang, Malaysia; and COMM2 from R&M Chemicals, Petaling Jaya, Malaysia). The preparation of CMC solutions to fully dissolve the CMC powder depended on the polymer concentration and temperature. Consequently, aqueous CMC solutions were prepared by dissolving the appropriate amount of CMC in distilled water at room temperature. The rheological behavior of CMC solutions at 1% and 4% concentrations were studied. The CMC solutions were prepared by hydrating them in distilled water overnight followed by vigorous hand mixing and then standing for 24 h to release air bubbles. The test samples were then gently and carefully mixed before measurements were taken to avoid air entrapment (Benchabane and Bekkour 2008).

All of the rheological measurements were performed on a controlled stress rheometer (AR-G2 TA Instruments, Malvern, UK) with a parallel plate configuration, where the sample was placed between a 20-mm stainless steel top flat plate and rheometer

Peltier base at a controlled temperature 20.0 °C ± 0.1 °C. To minimize the sensitivity of the CMC solution due to shear deformation history (possibility of time-dependent behavior), the solutions were gently stirred for 1 h before the samples were carefully loaded to the Peltier base. The top flat plate was then lowered at a very slowly to prevent the disruption of the solution structure. The samples were left to rest for 10 min prior to the measurements. A solvent trap was used to prevent evaporation of the samples during testing.

The rheometry mode used was steady-state flow for a low concentration at 1% and a high concentration at 4% for the CMC solutions. The flow curve of samples provided the correlation between the allocated shear stress and the resulting shear rate. The flow curve was plotted over a log-log scale with a shear rate from 0.1 s^{-1} to 1000 s^{-1} for both of the concentrations. Meanwhile, the viscosity curves portrayed the behavior of viscosity with increasing shear rates. The curves are plotted over a log-log scale of shear rate from 0.01 s^{-1} to 100 s^{-1} for the 1% CMC solution and 0.1 s^{-1} to 1000 s^{-1} for the 4% CMC solution.

RESULTS AND DISCUSSION

Lignocellulosic Composition

Figure 1 shows the lignocellulosic compositions of raw OPEFB stalk fibres, bleached OPEFB stalk fibres, OPEFB stalk α-cellulose, extracted carboxymethyl cellulose from OPEFB stalk fibres (SCMC), and the comparison with commercial CMC (COMM1 and COMM2).

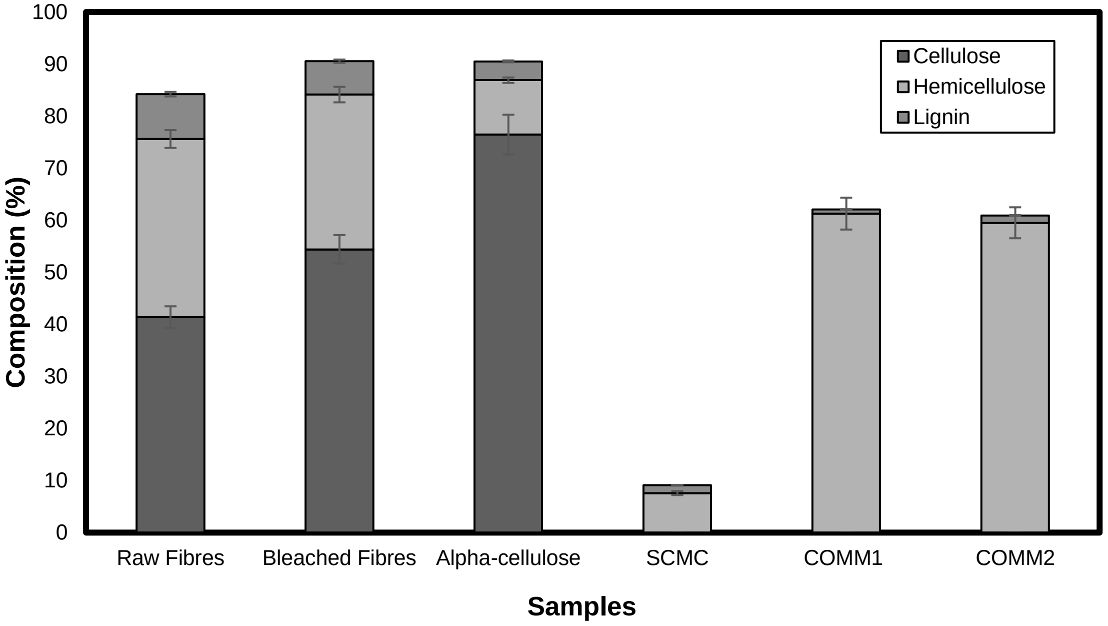

Fig. 1. Lignocellulosic composition of raw OPEFB stalk fibre, bleached OPEFB stalk fibre, OPEFB stalk α-cellulose, extracted OPEFB stalk CMC (SCMC), COMM1, and COMM2

The untreated stalk fibres contained a higher amount of lignin at 8.62% and hemicellulose at 29.73%. A slight change in the amount of lignin at 3.62% and hemicellulose at 34.21% was shown by the bleached fibres' results. A 6.41% reduction in lignin and 7.59% reduction in hemicellulose was observed in the α-cellulose OPEFB stalks, which implied that the alkali treatment was capable of removing the lignin and hemicellulose. Likewise, after the etherification process, there was 1.51% of lignin and 10.45% of hemicellulose left in the SCMC. The cellulose was completely substituted by the carboxyl group through the etherification process due to the reaction of the α-cellulose with monochloroacetate (MCA).

A large amount of cellulose at 76.45% was produced during the stage of cellulose extraction, and a notable reduction in the lignin and hemicellulose content was observed throughout the extraction process. Meanwhile, the lignocellulosic compositions of the SCMC was compared to local commercial CMC from Warisnove, Pahang, Malaysia (COMM1) and well-known commercial CMC from R&M Chemicals, Petaling Jaya, Malaysia (COMM2). The lignin percentage of the extracted SCMC was almost the same with the lignin percentages of COMM1 and COMM2, which are (1.51%, 0.78% and 1.41% respectively). The hemicellulose (10.45%) percentage of the extracted SCMC was much lower when compared to the hemicellulose in COMM1 and COMM2 (61.28% and 59.51%, respectively), which was due to the different source of fibres and the method that was used to produce the respective CMC. The complete removal of cellulose can be seen from SCMC and the commercial CMC because of the etherification process that converted cellulose to carboxymethyl cellulose through the substitution reaction of a carboxyl group.

XRD Analysis

The crystallinity level in polymers can be measured *via* X-ray diffraction (XRD) analysis. Figure 2 shows the XRD spectra at different stages during the production of OPEFB stalk CMC (SCMC) and the comparison with commercial CMC (COMM1 and COMM2).

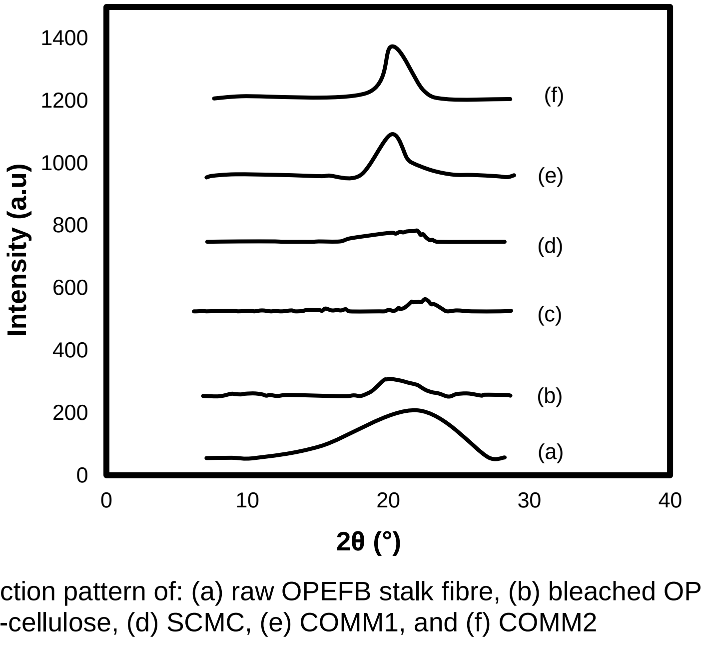

Fig. 2. X-ray diffraction pattern of: (a) raw OPEFB stalk fibre, (b) bleached OPEFB stalk fibre, (c) OPEFB stalk α-cellulose, (d) SCMC, (e) COMM1, and (f) COMM2

The peaks correspond to the crystalline amount, while the background corresponds to the amorphous amount. From the results obtained, it was observed that raw OPEFB stalk fibres demonstrated a broadened diffractions peak due to the crystalline structure of the fibre itself. The diffraction patterns showed the elimination of the crystalline composition number throughout the extraction process of SCMC. It was notable that the cellulose was semi-crystalline in nature. The diffraction peaks that appeared for the α-cellulose of OPEFB stalks nearly disappeared when compared to the raw OPEFB stalk fibre and bleached OPEFB stalk fibre because further treatment by using sodium hydroxide was completed to remove the lignin and hemicellulose. The extensive peaks corresponded to small crystallites in the cellulose granules. The diffraction arrangement of extracted SCMC showed a reduction in the crystalline structure from the native cellulose. All of the characteristic peaks for the original cellulose nearly disappeared and were converted into an amorphous phase. Thus, CMC has excellent solubility (Zhang and Wu 1992) as lower crystallinity represents higher solubility (He *et al.* 2009).

The CrI of the raw OPEFB stalk fibre was 72.8%, for the bleached OPEFB stalk fibres it was 88.6%, and for the α-cellulose of OPEFB stalks it was 56.8%. The withdrawal of lignin and hemicellulose, which were amorphous in nature, caused a considerable increase in the CrI after the bleaching process (Ramli *et al.* 2013). The FTIR results showed that the absence of the lignin and hemicellulose characteristic peaks marked that the components were greatly removed after it was chemically treated. Because cellulose is considered to be semi-crystalline in nature, the crystallinity index was reduced to 56.8%, which was approaching amorphous characteristics. The cellulose molecules treated in the alkaline medium during the carboxymethylation process caused swelling in the cellulose particles that exerted pressure on the crystalline part in the cellulose molecules in the vicinity and favorably distorted them. The dissociation and the distortion of the crystalline part caused by further swelling of cellulose molecules further reduces the crystallinity to 45.0% for SCMC (Fang *et al*. 2002). Previous studies showed a comparable crystallinity index of CMC at 38.3% (Mario *et al.* 2005) and 47.7% (Yanmei *et al.* 2012).

In Fig. 2, the crystalline peaks of COMM1 and COMM2 appeared to be sharper when compared to the extracted CMC from OPEFB stalks. The large percentage difference was due to the different procedures and sources used to obtain the CMC.

FTIR Analysis

The FTIR analysis was conducted to check the removal of lignin and hemicellulose. Figure 3 shows the FTIR spectra at different stages, which began with the untreated fibres until the final step that produced the OPEFB stalk CMC (SCMC), and the comparison with commercial CMC (COMM1 and COMM2). It was observed that the spectra between each step were remarkably different, indicating that chemical changes occurred throughout the extraction process.

In Fig. 3, the detected broad absorbance peaks in the range of 3500 cm^{-1} to 3200 cm^{-1} for all of the samples indicated free O-H stretching vibration, inter-molecular hydrogen bonds in cellulose molecules, and intra-molecular hydrogen bonds in cellulose molecules. However, the peaks that appeared at 2900 cm^{-1} to 2800 cm^{-1} were attributed to the bending of the aliphatic saturated C-H in lignin, hemicellulose, and cellulose. Abraham *et al.* (2011) mentioned that a strong cellulose-water interaction made the cellulose difficult to be dried entirely, even though all of the samples were subjected to the drying process before the FTIR analysis.

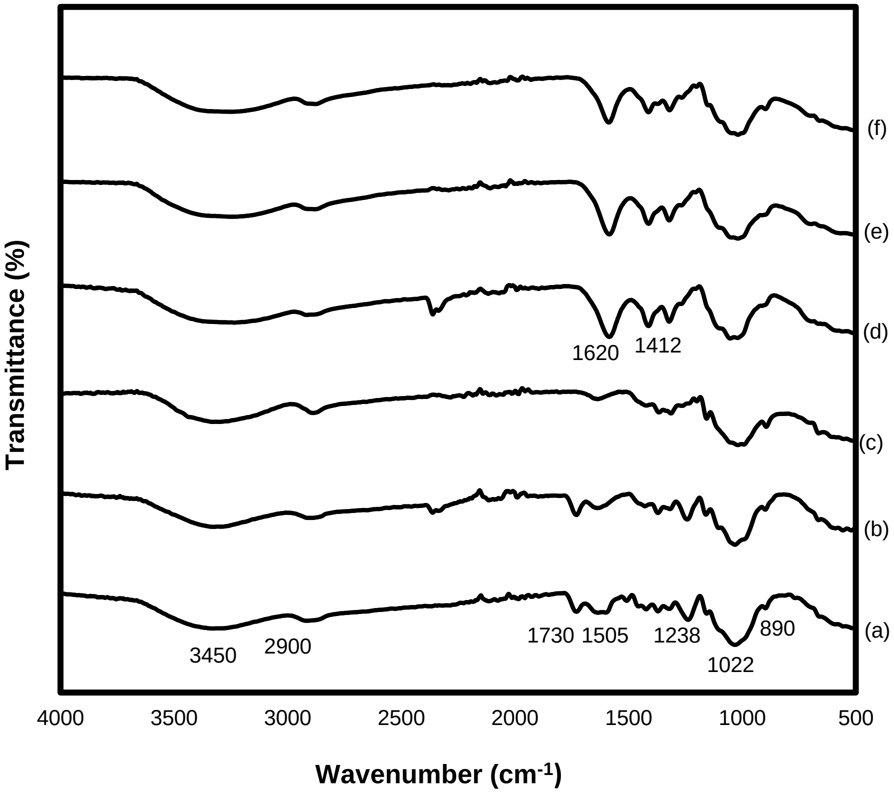

Fig. 3. FTIR spectra of (a) raw OPEFB stalk fibre, (b) bleached OPEFB stalk fibre, (c) OPEFB stalk α-cellulose, (d) SCMC, (e) COMM1, and (f) COMM2

There were few changes that formed between an 1800 cm^{-1} to 1000 cm^{-1} band range throughout the extraction process. Two characteristic peaks of lignin located at 1505 cm^{-1} (C=C stretching of aromatic ring of lignin) (Yunos *et al.* 2012) and at 1300 cm^{-1} to 1200 cm^{-1} corresponded to the C-O stretching of the aryl group in lignin were found in the spectra of the raw OPEFB stalk fibres (Abraham *et al.* 2011). This shows that the lignin was removed after the acidic bleaching. The alkali treatment process was based on the disappearance of the peak at 1505 cm^{-1} and the decrease in the peak intensity at 1300 cm^{-1} to 1200 cm^{-1} in α-cellulose of the OPEFB stalk spectra and the SCMC. Simultaneously, the C=O stretching that represented carboxylic acids, aldehyde, or ketone in hemicellulose appeared in the region of 1730 cm^{-1} to 1720 cm^{-1} in the untreated and bleached OPEFB stalk fibres (Fahma *et al.* 2010; Yunos *et al.* 2012). The withdrawal of lignin and hemicellulose after the extraction resulted in the disappearance of the particular peak from the spectra in the α-cellulose and the SCMC from the OPEFB stalk fibres.

Specific types of absorption bands at 1730 cm^{-1}, 1505 cm^{-1}, and 1238 cm^{-1} were not observed in the α-cellulose of the OPEFB stalk. Particularly, the bands at 1505 cm^{-1} and 1238 cm^{-1} must be emphasized. The band at 1505 cm^{-1} no longer existed, and the band at 1238 cm^{-1} decreased exceedingly in the α-cellulose of OPEFB stalk spectra because most of the lignin had been removed (Khalil *et al.* 1990; Bhattacharyya *et al.* 1995). The disappearance of the peak at 1730 cm^{-1} demonstrated that the hemicellulose had been removed.

Furthermore, all of the samples from the beginning of the extraction process in the OPEFB stalk of the CMC similarly exhibited the common characteristic peaks in the cellulose components. The visible peak at 890 cm^{-1} was attributed to the links in the β-glycosidic that held the glucose units in the cellulose (Azubuike and Okhamafe 2012). The elimination of lignin and hemicellulose that surrounded the cellulose fibrils made the contrast between the peaks associated with the raw fibres and those of the synthesized CMC more apparent. Moreover, the peak perceived at 1238 cm^{-1} was assigned to the C-H bond stretching vibration of cellulose (Nazir *et al.* 2013), while Elanthikkal *et al.* (2010) found that the peak at 1022 cm^{-1} was associated to the skeletal vibration of the C-O-C pyranose ring. The withdrawal of the hemicellulose and lignin parts made the peaks of the raw fibres spectra become notable, and the peaks became more appealing after the extraction process was completed.

The comparison in the infrared spectra with extracted OPEFB stalk CMC (SCMC), COMM1 CMC, and COMM2 CMC samples is shown in Fig. 4. The existence of a new and prominent wavenumber at 1620 cm^{-1} affirmed the stretching frequency of carboxyl groups (COO-), and the value of 1412 cm^{-1} was attributed to carboxyl groups as salts (Biswal and Singh 2004; Bono *et al.* 2009). The IR spectra sequences of COMM1 and COMM2 were almost similar with the extracted SCMC.

To summarize, the bleaching of acidified $NaClO_2$ followed by a NaOH (alkali) treatment was suitable for use to remove the hemicellulose and lignin components, which were considered to be the major non-cellulosic components in the raw OPEFB stalk fibres. The elimination of hemicellulose and lignin components was affirmed by the disappearance in the characteristic peaks in hemicellulose (1730 cm^{-1} to 1720 cm^{-1}) and lignin (1505 cm^{-1} and 1300 cm^{-1} to 200 cm^{-1}) in the synthesized SCMC. In addition, the existence of the carboxymethyl ether group (1620 cm^{-1}) confirmed that monochloroacetate used for etherification process led to the substitution of the carboxyl groups with the carboxymethyl ether group, as the α-cellulose was converted to CMC.

Microstructural Analysis

Figure 4 shows images of the different stages that were involved in the extraction process of SCMC, where a comparison with COMM1 and COMM2 was analyzed by SEM. Similarly, Xiang *et al.* (2015) reported that excessive lignin and waxes were apparent on the raw OPEFB stalk fibre.

The bleaching process that involved acidified $NaClO_2$ generated the empty cavities and pores due to the withdrawal of silica bodies, as shown in Fig. 4(b). The fibril strands were exposed because the external layer of the bleached fibre was distorted and ruptured. The chlorite bleaching process led to the removal of the lignin component, so that it provided impermeability, rigidity, and protection to the structure of the lignocellulosic biomass (Kumar *et al.* 2009).

Smaller fibre bundles, which can be observed in Fig. 4(c), were individually detached from the fibre bundles after undergoing treatment with 17.5% (v/v) NaOH. The fibre bundles containing highly purified α-cellulose fibrils were due to the removal of hemicellulose and lignin. The exterior surface of the cellulose showed rough fibers that were twisted and ruptured, which may have been caused by the use of strong chemicals and high temperature in the cellulose extraction process. For SCMC, the roughness was slightly decreased when compared to cellulose; the results were consistent with a process in which the cellulose crystallinity that was changed to allow the etherifying agent to have access to the cellulose molecule (Rachatanapun *et al.* 2012).

For comparison purposes, Figs. 4(e) and 4(f) show the microstructural images of the COMM1 and COMM2. The COMM1 and COMM2 showed a smooth and dense surface compared to the extracted SCMC Fig. 4(d). Both of the commercial CMC samples showed a short strand compared to SCMC, which had long and narrow strand characteristics.

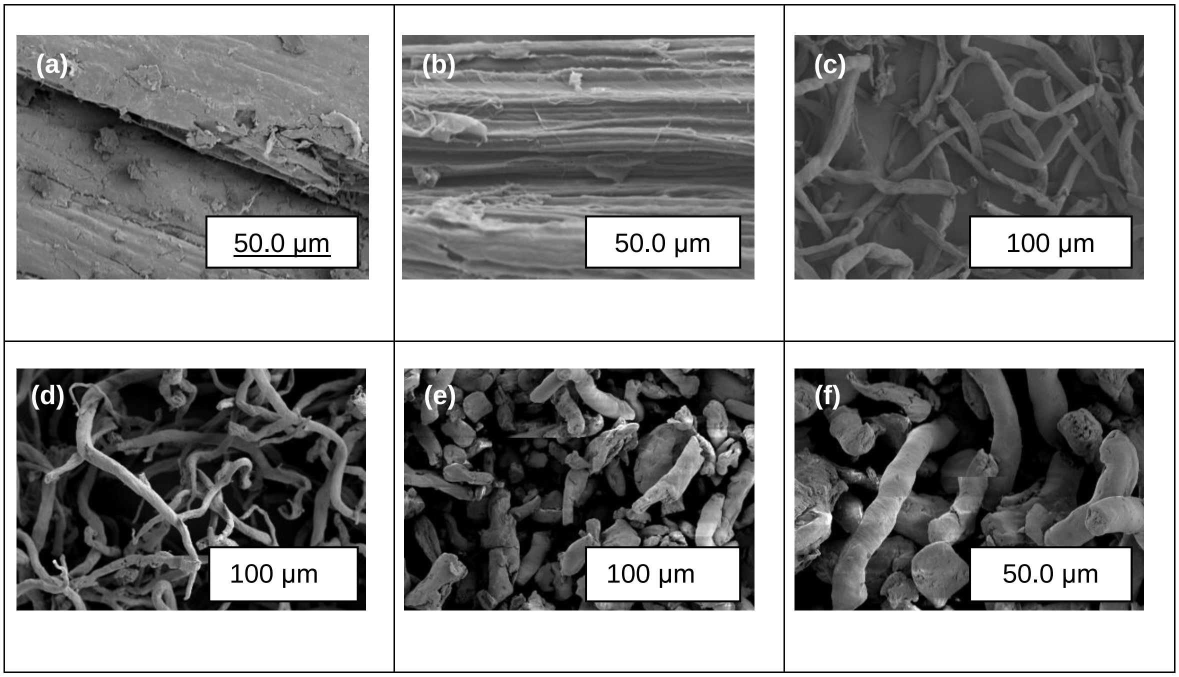

Fig. 4. SEM images of (a) raw OPEFB stalk fibre, (b) bleached OPEFB stalk fibre, (c) OPEFB stalk α-cellulose, (d) SCMC (e) COMM1 and (f) COMM2

Physicochemical Properties of Synthesized Na-CMC

The proportion of active polymers in a substance is an important measure to be determined to perceive the amount of CMC to use in different formulations. Thus, a moisture content analysis was conducted to calculate the total solids in the sample; all volatile substance at this test temperature were accounted as moisture.

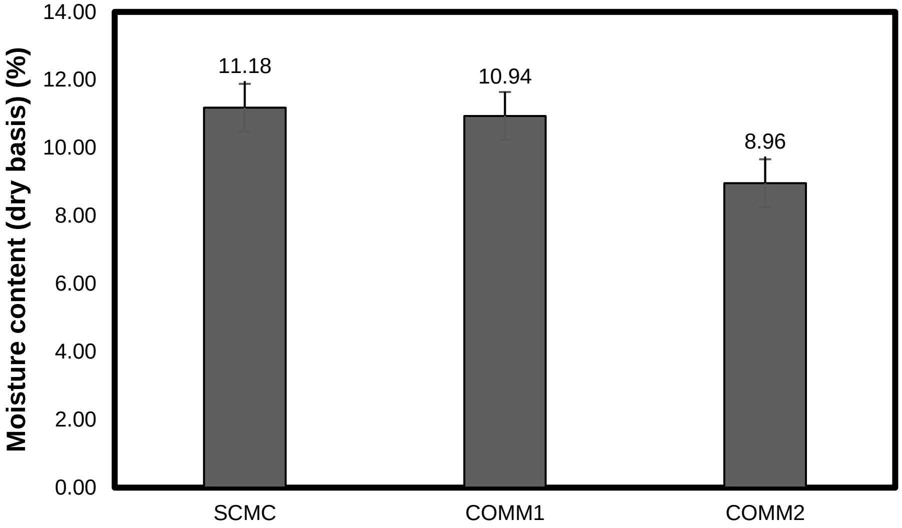

Fig. 5. Moisture content of SMCC, COMM1, and COMM2

In Fig. 5, the mean moisture content of SCMC was 11.2%, COMM1 was 10.9%, and COMM2 was 9.0%. The moisture content of SCMC was comparable to the commercial CMC and it had the highest moisture content.

According to standard procedure (FAO/WHO Expert Committee 2011), the moisture content of CMC should not be higher than 12%. From the results obtained, the SCMC was considered pure because it was within the maximum moisture content (%) allocated for the CMC standard requirement. In general, the moisture content of CMC will also affect the flowability when the CMC is in powder form. Powder with higher moisture content will reduce its ability to flow smoothly (Fitzpatrick *et al.* 2004). The experimental values of true, bulk, and tapped density are tabulated in Table 1.

Table 1. Densities of SCMC, COMM1, and COMM2

Materials			
Densities	**SCMC**	**COMM1**	**COMM2**
Bulk Density (g/cm^3)	0.325 ± 0.008	0.496 ± 0.002	0.498 ± 0.002
Tapped Density (g/cm^3)	0.472 ± 0.001	0.634 ± 0.010	0.569 ± 0.012
True Density (g/cm^3)	1.254 ± 0.005	1.463 ± 0.001	1.457 ± 0.001

Based on the data tabulated in Table 1, the bulk, tapped, and true density for SCMC had the lowest values compared to COMM1 and COMM2. Meanwhile, both types of commercial CMC showed nearly the same values for the bulk and true density, but a slight difference in the tapped density value.

The insufficient fine particles to fill in the empty space between the slit of bulk particles was clearly the reason for the lower value in the tapped density perceived from the SCMC. The continuous tapping method could not remove the fine particles from the larger particles because it was presumed that the fine particles within the samples surrounded the larger particles (Abdullah and Geldart 1999). The flowability of the powders was determined according to the Hausner ratio (HR) and Carr index (CI) that were determined. The values of the HR and CI for each type of CMC sample are shown in Figs. 6 and 7, respectively.

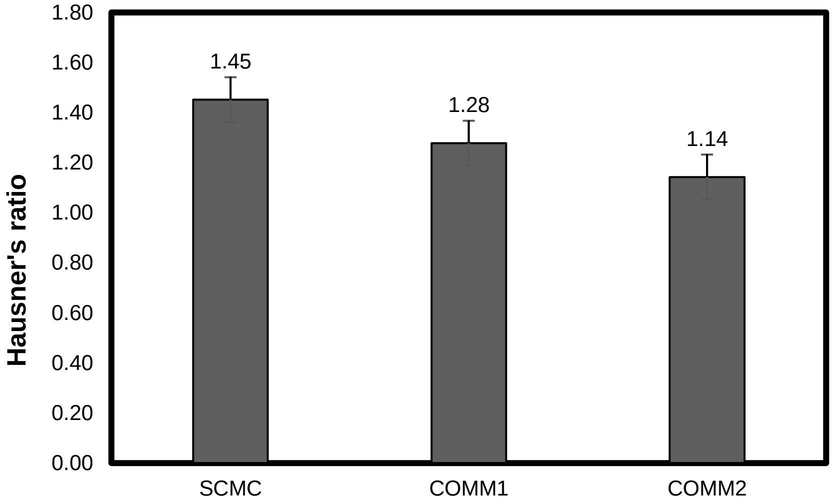

Fig. 6. Hausner ratio of SCMC, COMM1, and COMM2

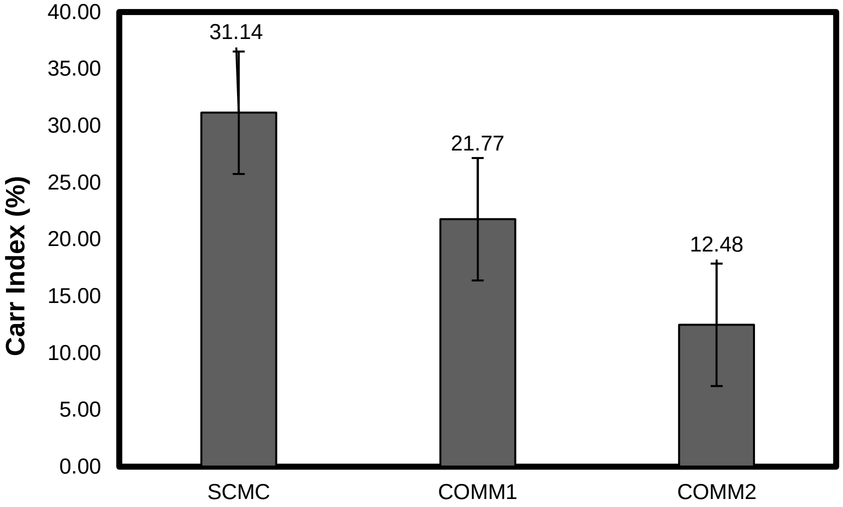

Fig. 7. Carr index of SCMC, COMM1, and COMM2

As shown in Fig. 6, COMM2 had the lowest HR value of 1.14 when compared to the other two CMC. The value of HR for COMM1 was 1.28, whereas the SCMC showed the highest value, which was 1.45. Moreover, Fig. 8 shows the CI for each type of CMC powder. Based on Fig. 7, COMM2 had the lowest value for Carr index (12.5%), whereas the CI for COMM1 was 21.8%. Meanwhile, the SCMC had the highest value of CI, which was 31.1%.

Table 2. Flow Character for CMC Samples

Materials	Carr Index (%)	Hausner's Ratio	Flow Character
SCMC	31.14	1.452	Very poor
COMM1	21.77	1.278	Passable
COMM2	12.48	1.143	Good

Therefore, the flow character for each type of CMC powder was concluded to be shown in Table 2. The COMM2 was considered as a ‘good’ flow character, as its HR was between Scale 1.12 to Scale 1.18 and the CI value was between 11% to 15%. Moreover, the COMM1 was judged as a passable flow because its HR value was between Scale 1.26 to Scale 1.34 and its CI was between 21% to 25%. Furthermore, SCMC was considered to have very poor flow because its HR was between Scale 1.46 to Scale 1.59 and its CI was between 32% to 37%. As previously mentioned, a higher moisture content will affect the flowability of the CMC powders (Crouter and Briens 2014).

The experimental values for the water retention capacity of each type of CMC powder are shown in Fig. 8. The water retention capacity values for both and COMM2 were 21.7. In contrast, the SCMC had the lowest value of WRC, 21.5. In general, the high WRC for COMM2 implied that this type of CMC was highly hydrophilic. This may have been due to the etherification process when there were more carboxymethyl groups, which is when the hydrophillic substituted the hydroxyl groups (Mondal *et al.* 2015). The values of L^*, a^*, and b^* for each type of CMC powder are tabulated in Table 3.

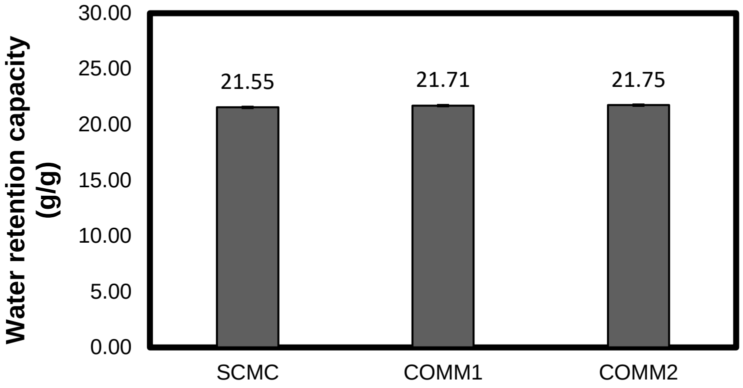

Fig. 8. Water retention capacity of SCMC, COMM1, and COMM2

Table 3. Values of *L*, *a*, and *b* for Each Type of CMC Powder

Materials	*L*	*a*	*b*
SCMC	96.57 ± 0.18	-0.70 ± 0.09	5.14 ± 0.28
COMM1	92.85 ± 0.09	0.61 ± 0.03	7.50 ± 0.02
COMM2	93.90 ± 0.05	0.36 ± 0.00	5.34 ± 0.06

As shown, SCMC had the higher lightness in color compared to the other two types of CMC powders. The highest *L* value indicated a lighter color (Hunterlab 2012). However, the SCMC were slightly green in color, since the *a* value was negative. The negative *a* value indicated the green color of the materials, whereas the positive *a* value indicated the redness color of the materials (Hunterlab 2012). In addition, the SCMC was slightly yellow in color, as it had a positive *b* value. The positive *b* value indicated the yellowness and the negative *b* value indicated the blueness of the materials. Thus, it was shown that SCMC was colorless based on the values of *L*, *a*, and *b* that were obtained.

Table 4. OPEFB Stalk CMC (SCMC) Parameters

pH in 1% Solution	Scale 6 to 8
Solubility	Forms viscous solution with water but insoluble in ethanol
Organoleptic	Odorless, milky white, free flowing powder
Foam	No layer of foam appears by shaking in 0.1% solution

Table 1 shows the physicochemical test outcomes of the extracted SCMC acquired from the OPEFB stalk fibre. The pH of the 1% CMC solution was in the range 6 to 8. The 0.1% CMC solution revealed no layer of foam after shaking was completed. This test indicates that the extracted SCMC was different from other natural gums, cellulose ethers, and alginates.

Rheological Behavior

The results of the flow behavior for the 1% low concentration and 4% high concentration of CMC solutions are shown in Fig. 9. The correlation between the allocated shear stress and the resulting shear rate provided the flow curve of the samples in the controlled stress system. In addition, the behavior of the viscosity with increasing shear rates illustrated the viscosity curves.

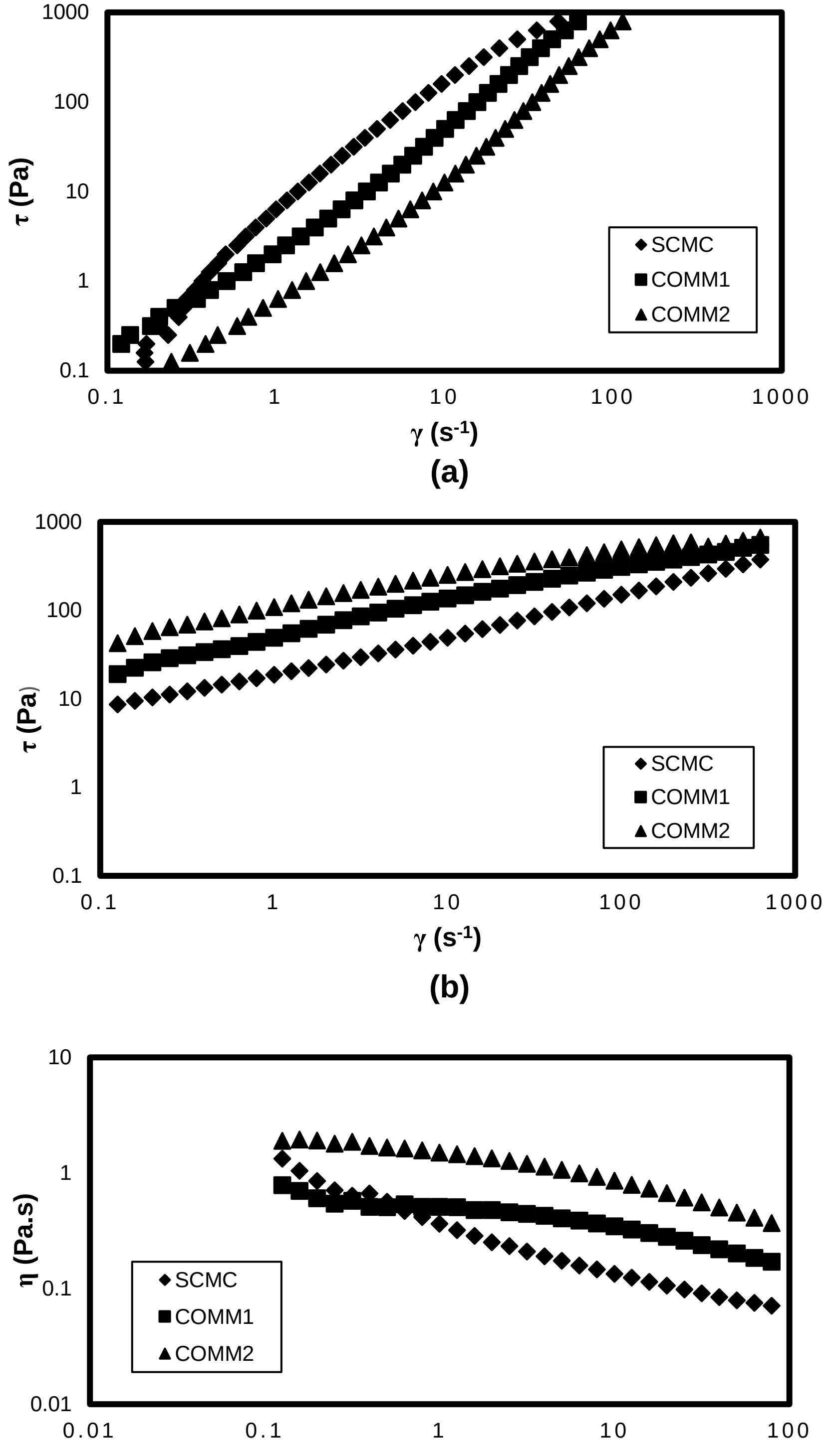

(a)

(b)

(c)

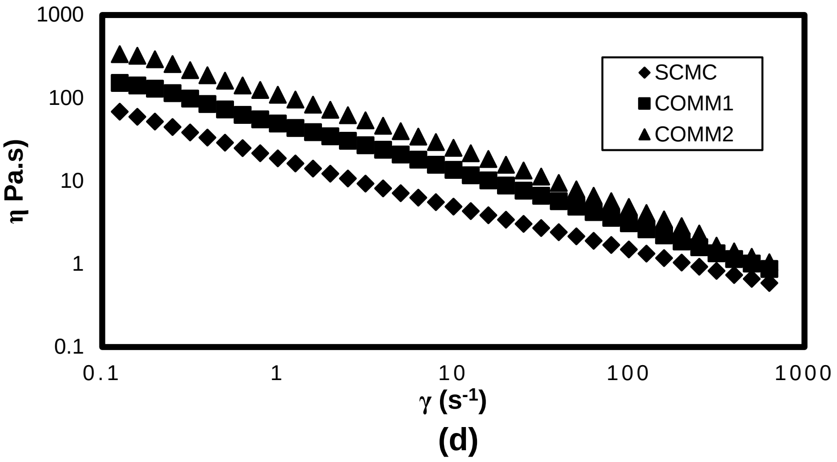

Fig. 9. Flow behavior curves of SCMC, COMM1, and COMM2 solutions at: (a) 1% CMC solution, (b) 4% CMC solution, and viscosity as a function of shear rate for CMC solutions at (c) 1% CMC solution, and (d) 4% CMC solution

The flow curves of the shear stress-shear rate relationships of SCMC, COMM1, and COMM2 with 1% concentration are depicted in Fig. 10(a). Meanwhile, the flow curves of shear stress-shear rate relationships of SCMC, COMM1, and COMM2 with 4% concentration are illustrated in Fig. 10(b). The cycles of the shear rate ranging from 0.1 s^{-1} to 1000 s^{-1} were plotted in the log-log scale curves for both concentrations. All of the CMC samples in the 1% and 4% of CMC solutions displayed a consistent almost linear curve pattern.

Figures 10(c) and 10(d) show a strong pseudoplastic behavior for the SCMC, 1% concentration of commercial CMC, and 4% concentration of commercial CMC. The curves are plotted over a log-log scale of shear rate from 0.01 s^{-1} to 100 s^{-1} for the 1% CMC solution and 0.1 s^{-1} to 1000 s^{-1} for the 4% CMC solution. In practice, at higher shear rates, the flow encountered less resistance. The CMC solutions with a higher value of viscosity, which was attributed to an irregular interior order that structured a high resistance against flow due to its long entangled and looping molecular chains. The chain type molecules in CMC solutions were stretched, disentangled, and reoriented parallel to the driving force when the shear rates were increased. The viscosity of the CMC solutions decreased because the molecular aligning enabled molecules to simply slip past each other (Mamdouh *et al.* 1997).

CONCLUSIONS

The extraction of cellulose from OPEFB stalks fibre was achieved through conventional delignification or bleaching technique by using acidic sodium chlorite solution and sodium hydroxide. Based on the study, the findings obtained were:

1. The CMC obtained from the infusion of cellulose-OPEFB stalks fibre with NaOH and monochloroacetate showed consistent results with commercial CMC (COMM1 and COMM2) indicated by the complete substitution of cellulose with reduction in crystallinity index of SCMC to 45%.

2. The chemical configuration of carboxyl group of SCMC by FTIR analysis at 1620 cm^{-1} (carboxyl groups COO-) and 1412 cm^{-1} (attributed to carboxyl groups as salts) were comparable with both of the commercial CMC specimens considered.
3. The extracted CMC showed a moisture content of 11.2%, with low value of water retention capacity of 21.5, which is on a par with both commercial CMC.
4. In the rheological testing, at 1% and 4% of all CMC solutions (SCMC, COMM1 and COMM2) exhibit a similar linear curve pattern for flow behavior and viscosity curve, indicating good quality of SCMC and comparable with both commercial CMC.

The findings of this study are intended to provide an in-depth understanding of the behavior of CMC extracted from OPEFB stalks fibre and to facilitate further exploration of the potential CMC synthesis from other agricultural biomass resources. The less contaminated OPEFB stalk makes it a great raw material to be used in producing more value-added products for food applications.

ACKNOWLEDGMENTS

The authors were grateful for the support from the laboratory staff that helped in handling the equipment for the analyses involved in the research. This study was done in the laboratory of Process and Food Engineering, Faculty of Engineering, Universiti Putra Malaysia.

REFERENCES CITED

Abraham, E., Deepa, B., Pothan, L. A., John, M. J., Thomas, S., Anandjiwala, R., and Cvelbar, U. (2011). “Extraction of nanocellulose fibrils from lignocellulosic fibres – A novel approach,” *Carbohydrate Polymers* 86(4), 1468-1475. DOI: 10.1016/j.carbpol.2011.06034

Adinugraha, M. P., Marseno, D. W., and Haryadi (2005). “Synthesis and characterization of sodium carboxymethylcellulose from cavendish banana pseudo stem (*Musa cavendishii* LAMBERT),” *Carbohydrate Polymers* 62(2), 164-169. DOI: https://doi.org/10.1016/j.carbpol.2005.07.019

ASTM D1439-03 (2008). “Standard test methods for sodium carboxymethylcellulose,” ASTM International, West Conshocken, PA.

Azubuike, C. P., and Okhamafe, A. O. (2012). “Physicochemical, spectroscpic and thermal properties of microcrystalline cellulose derived from corn cobs,” *International Journal of Recycling Organic Waste in Agriculture* 1(1), 9. DOI: 10.1186/2251-7715-1-9

Benchabane, A., and Bekkour, K. (2008). “Rheological properties of carboxymethyl cellulose solutions,” *Colloid Polymer Science* 286, 1173-1180. DOI: 10.1007/s00396-008-1882-2

Bhattacharyya, D., Singhal, R. S., and Kulkarni, P. R. (1995). “A comparative account of conditions for synthesis of sodium carboxymethyl starch from corn and amaranth starch," *Carbohydrate Polymers* 27(4), 247-253. DOI: 10.1016/0144-8617(95)00083-6

Biswal, D. R., and Singh, R. P. (2004). "Characterisation of carboxymethyl cellulose and polyacrylamide graft copolymer," *Carbohydrate Polymers* 57(4), 379-387. DOI: 10.1016/j.carbpol.2004.04.020

Bono, A., Ying, P. H., Yan, F. Y., Muei, C. L., Sarbatly, R., and Krishnaiah, D. (2009). "Synthesis and characterization of carboxymethyl cellulose from palm kernel cake," *Advances in Natural and Applied Sciences* 3(1), 5-11.

Crouter, A., and Briens, L. (2014). "The effect of moisture on the flowability of pharmaceutical excipients," *AAPS PharmSciTech* 15(1), 65-74. DOI: 10.1208/S12249-013-0036-0

Elanthikkal, S., Gopalakrishnapanicker, U., Varghese, S., and Guthrie, J. T. (2010). "Cellulose microfibres produce from banana plant wastes: Isolation and characterization," *Carbohydrate Polymers* 80(3), 852-859. DOI: 10.1016/j.carbpol.2009.12.043

Fahma, F., Iwamoto, S., Hori, N., Iwata, T., and Takemura, A. (2010). "Isolation, preparation, and characterization of nanofibers from oil palm empty fruit bunch," *Cellulose* 17(5), 977-985. DOI: 10.1007/s10570-010-9436-4

Fang, J. M., Fowler, P.A., Tomkinson, J., and Hill, C. A. S. (2002). "The preparation and characterisation of a series of chemically modified potato starches," *Carbohydrate Polymers* 47(3), 245-252. DOI: 10.1016/S0144-8617(01)00187-4

FAO/World Health Organization (WHO) Expert Committee (2011). *Compendium of Food Additive Specifications*, Food and Agriculture Organization of the United Nations, Rome, Italy.

Fitzpatrick, J. J., Barringer, S. A., and Iqbal, T. (2004). "Flow property measurement of food powders and sensitivity of Jenike's hopper design methodology to the measured values," *Journal of Food Engineering* 61, 399-405. DOI: 10.1016/S0260-8774(03)00147-X

He, X., Wu, S., Fu, D., and Ni, J. (2009). "Preparation of sodium carboxymethyl cellulose from paper sludge," *Journal of Chemical Technology and Biotechnology* 84(3), 427-434. DOI: 10.1002/jctb.2057

Hunterlab (2012). *Measuring Color Using Hunter L, a, b Versus CIE 1976 L*a*b**, Hunter Associates Laboratory Inc., Reston, VA, USA.

Kumar, P., Barrett, D. M., Delwiche, M. J., and Stroeve, P. (2009). "Methods for pretreatment of lignocellulosic biomass for efficient hydrolysis and biofuel production," *Industrial and Engineering Chemistry Research* 48(8), 3713-3729. DOI: 10.1021/ie801542g

Khalil, M. I., Hasem, A., and Habeish, A. (1990). "Carboxymethylation of maize starch," *Starch* 42(2), 60-63. DOI: 10.1002/star.19900420209

Larrauri, J. A., Ruperez, P., Borroto, B., and Saura-Calixto, F. (1996). "Mango peels as a new tropical fibre – Preparation and characterization," *LWT- Food Science and Technology* 29(8), 729-733. DOI: 10.1016/S0144-8617(01)00187-4

Mamdouh, T. G., and Esmail, M. N. (1997). "Rheological properties of carboxymethyl cellulose,"*Journal of Applied Polymer Science* 64(2), 289-301. DOI: 10.1002/(SICI)1097-4628(19970411)64:2<289::AID-APP9>3.0.CO;2-N

Mario, P. A., Djagal, W. M., and Haryadi (2005). "Synthesis and characterization of sodium carboxymethylcellulose from cavendish banana psuedo stem (*Musa* *cavendishii)*," *Carbohydrate Polymers* 62, 164-169. DOI: 10.1016/j.carbpol.2005.07.019

Mohammed, M. A. A., Salmiaton, A., Wan Azlina, W. A. K. G., and Mohamad Amran, M. (2012). "Gasification of oil palm empty fruit bunches – A characterization and kinetic study," *Bioresource Technology* 110, 628-636. DOI: 10.1016/j.biortech.2012.01.056

Mondal, M. I. H., Yeasmin, M. S., and Rahman, M. S. (2015). "Preparation of food grade carboxymethyl cellulose from corn husk agrowaste," *International Journal of Biological Macromolecules* 79, 144-150. DOI: 10.1016/j.ijbiomac.2015.04.061

Nazir, M. S., Wahjoedi, B. A., Yussof, A. W., and Abdullah, M. A. (2013). "Eco-friendly extraction and characterization of cellulose from oil palm empty fruit bunches," *BioResources* 8(2), 2161-2172. DOI: 10.15376/biores.8.2.2161-2172

Pushpamalar, V., Langford, S. J., Ahmad, M., and Lim, Y. Y. (2006). "Optimization of reaction conditions for preparing carboxymethyl cellulose from sago waste," *Carbohydrate Polymers* 64(2), 312-318. DOI: 10.1016/j.carbpol.2005.12.003

Rachatanapun, P., Luangkamin, S., Tanprasert, K., and Suriyatem, R. (2012). "Carboxymethyl cellulose film from durian rind," *Food Science and Technology* 48(1), 52-58. DOI: 10.1016/j.lwt.2012.02.029

Ramli, R., Junadi, N., Beg, M. D. H., and Abdullah, M. A. (2013). "Microcrystalline cellulose from oil palm empty fruit bunch fiber *via* simultaneous ultrasonic and alkali treatment," *International Journal of Chemical, Nuclear, Materials, and Metallurgical Engineering* 8(2), 8-11.

Razali, N., Hossain, M. S., Taiwo, O. A., Ibrahim, M., Nadzri, N. W. M., Razak, N., and Kassim, M. H. M. (2017). "Influence of acid hydrolysis reaction time on the isolation of cellulose nanowhiskers from oil palm empty fruit bunch microcrystalline cellulose," *BioResources* 12(3), 6773-6788. DOI: 10.15376/biores.12.3.6773-6788

Tasaso, P. (2015). "Optimization of reaction conditions for synthesis of carboxymethyl cellulose from oil palm fronds," *International Journal of Chemical Engineering and Applications* 6(2), 101-104. DOI: 10.7763/IJCEA.2015.V6.460

Xiang, L. Y., Hanipah, S. H., Mohammed, M. A. P., Baharuddin, A. S., and Lazim, A. M. (2015). "Microstructural, mechanical, and physicochemical behaviours of alkali pre-treated oil palm stalk fibres," *BioResources* 10(2), 2783-2796. DOI: 10.15376/biores.10.2.2783-2796

Xiang, L. Y., Mohammed, M. A. P., and Baharuddin, A. S. (2016). "Characterisation of microcrystalline cellulose from oil palm fibres for food applications," *Carbohydrate Polymers* 148, 11-20. DOI: 10.1016/j.carbpol.2016.04.055

Yanmei, Z., Xiaoyi, H., Min, Z., Xiaofeng, Z., and Jingyang, N. (2012). "Preparation and characterization of modified cellulose for adsorption of Cd (II), Hg (II), and acid fuchsin from aqueous solutions," *Industrial and Engineering Chemistry Research* 52(2), 876-884. DOI: 10.1021/ie301742h

Yunos, N. S. H. M., Baharuddin, A. S., Yunos, K. F. M., Naim, M. N., and Nishida, H. (2012). "Physicochemical property changes of oil palm mesocarp fibers treated with high-pressure steam," *BioResources* 7(4), 5983-5994. DOI: 10.15376/biores.7.4.5983-5994

Yunos, N. S. H. M., Baharuddin, A. S., Yunos, K. F. M., Hafid, H. S., Busu, Z., Mokhtar, M. N., Sulaiman, A., and Md. Som, A. (2015). "The physicochemical characteristics of residual oil and fibers from oil palm empty fruit bunches," *BioResources* 10(1), 14-29. DOI: 10.15376/biores.10.1.14-29

Zhang, J., and Wu, D. (1992). “Characteristics of the aqueous solution of carboxymethyl starch ether,” *Journal of Applied Polymer Science* 46(2), 369-374. DOI: 10.1002/app.1992.070460218

Article submitted: September 6, 2017; Peer review completed: October 29, 2017; Revised version received: November 7, 2017; Accepted: November 8, 2017; Published: November 22, 2017.
DOI: 10.15376/biores.13.1.535-554